Wyoming Cloud Lidar: instrument description and applications

Zhien Wang*, Perry Wechsler, William Kuestner, Jeffrey French, Alfred Rodi, Brent Glover, Matthew Burkhart and Donal Lukens

Department of Atmospheric Science, University of Wyoming, Laramie, Wyoming, USA
** zwang@uwyo.edu*

Abstract: The Wyoming Cloud Lidar (WCL), a compact two-channel elastic lidar, was designed to obtain cloud measurements together with the Wyoming Cloud Radar (WCR) on the University of Wyoming King Air and the National Science Foundation/National Center of Atmospheric Research C-130 aircraft. The WCL has been deployed in four field projects under a variety of atmospheric and cloud conditions during the last two years. Throughout these campaigns, it has exhibited the needed reliability for turn-key operation from aircraft. We provide here an overview of the instrument and examples to illustrate the measurements capability of the WCL. Although the WCL as a standalone instrument can provide unique measurements for cloud and boundary layer aerosol studies, the synergy of WCL and WCR measurements coupled with in situ sampling from an aircraft provide a significant step forward in our ability to observe and understand cloud microphysical property evolution.

OCIS codes: (280.3640) Lidar; (290.1090) Aerosol and cloud effects; (290.5855) Scattering, polarization; (290.1350) Backscattering

References and links

1. B. A. Wielicki, R. D. Cess, M. D. King, D. A. Randall, and E. F. Harrison, "Mission to planet earth: role of clouds and radiation in climate," Bull. Am. Meteorol. Soc. **76**(11), 2125–2154 (1995).
2. IPCC, "Climate Change 2007 The Physical Science Basis. Contribution of Working Group I to the Fourth Assessment Report of the Intergovernmental Panel on Climate Change," Solomon, S., D. Qin, M. Manning, Z. Chen, M. Marquis, K.B. Averyt, M. Tignor and H.L. Miller eds. (Cambridge University Press, Cambridge, United Kingdom and New York, NY, USA, 996 pp, 2007).
3. R. D. Cess, M. H. Zhang, W. J. Ingram, G. P. Potter, V. Alekseev, H. W. Barker, E. Cohen-Solal, R. A. Colman, D. A. Dazlich, A. D. Del Genio, M. R. Dix, V. Dymnikov, M. Esch, L. D. Fowler, J. R. Fraser, V. Galin, W. L. Gates, J. J. Hack, J. T. Kiehl, H. Le Treut, K. K.-W. Lo, B. J. Mcavaney, V. P. Meleshko, J.-J. Morcrette, D. A. Randall, E. Roeckner, J.-F. Royer, M. E. Schlesinger, P. V. Sporyshev, B. Timbal, E. M. Volodin, K. E. Taylor, W. Wang, and R. T. Wetherald, "Cloud feedback in atmospheric general circulation models: An update," J. Geophys. Res. **101**(D8), 12791–12794 (1996).
4. S. Bony, and J.-L. Dufresne, "Marine boundary layer clouds at the heart of tropical cloud feedback uncertainties in climate models," Geophys. Res. Lett. **32**(20), L20806 (2005), doi:10.1029/2005GL023851.
5. G. Asrar, J. A. Kaye, and P. Morel, "NASA research strategy for earth system science: Climate component," Bull. Am. Meteorol. Soc. **82**(7), 1309–1330 (2001).
6. G. L. Stephens, D. G. Vane, R. J. Boain, G. G. Mace, K. Sassen, Z. Wang, A. J. Illingworth, E. J. O'Connor, W. B. Rossow, S. L. Durden, S. D. Miller, R. T. Austin, A. Benedetti, and C. Mitrescu, "The CloudSat mission and the A-TRAIN: A new dimension to space-based observations of clouds and precipitation," Bull. Am. Meteorol. Soc. **83**, 1771–1790 (2002).
7. T. Ackerman, and G. Stokes, "The Atmospheric Radiation Measurement Program," Phys. Today **56**(1), 38–45 (2003).
8. J. M. Fritsch, and R. E. Carbone, "Improving quantitative precipitation forecasts in the warm season: A USWRP research and development strategy," Bull. Am. Meteorol. Soc. **85**(7), 955–965 (2004).
9. P. H. Hildebrand, W. C. Lee, C. A. Walther, C. Frush, M. Randall, E. Loew, R. Neitzel, R. Parsons, J. Testud, F. Baudin, and A. LeCornec, "The ELDORA/ASTRAIA Airborne Doppler Weather Radar: High-Resolution Observations from TOGA COARE," Bull. Am. Meteorol. Soc. **77**(2), 213–232 (1996).

#110893 - $15.00 USD Received 4 May 2009; revised 19 Jun 2009; accepted 19 Jun 2009; published 23 Jul 2009

10. G. M. Heymsfield, S. W. Bidwell, P. Racette, I. J. Caylor, S. Ameen, S. Nicholson, W. Boncyk, L. Miller, D. Vandemark, and L. R. Dod, "The EDOP radar system on the high-altitude NASA ER-2 aircraft," J. Atmos. Ocean. Technol. **13**(4), 795–809 (1996).
11. D. Leon, G. Vali, and M. Lothon, "Dual-Doppler analysis in a single plane from an airborne platform. Part I: Technique," J. Atmos. Ocean. Technol. **23**(1), 3–21 (2006).
12. G. M. Heymsfield, J. M. Shepherd, S. W. Bidwell, W. C. Boncyk, I. J. Caylor, S. Ameen, and W. S. Olson, "Structure of Florida thunderstorms using high-altitude aircraft radiometer and radar observations," J. Appl. Meteorol. **35**(10), 1736–1762 (1996).
13. G. Vali, R. Kelly, J. French, S. Haimov, D. Leon, R. McIntosh, and A. Pazmany, "Finescale structure and microphysics of coastal stratus," J. Atmos. Sci. **55**(24), 3540–3564 (1998).
14. B. Stevens, D. H. Lenschow, G. Vali, H. Gerber, A. Bandy, B. Blomquist, J.-L. Brenguier, C. S. Bretherton, F. Burnet, T. Campos, S. Chai, I. Faloona, D. Friesen, S. Haimov, F. Laursen, D. K. Lilly, S. M. Loehrer, S. P. Malinowski, B. Morley, M. D. Petters, D. C. Rogers, L. Russell, V. Savic-Jovcic, J. R. Snider, D. Straub, M. J. Szumowski, H. Takagi, D. C. Thornton, M. Tschudi, C. Twohy, M. Wetzel, and M. C. van Zanten, "Dynamics and Chemistry of Marine Stratocumulus–DYCOMS-II," Bull. Am. Meteorol. Soc. **84**(5), 579–593 (2003).
15. R. Damiani, G. Vali, and S. Haimov, "The structure of thermals in cumulus from airborne dual-Doppler radar observations," J. Atmos. Sci. **63**(5), 1432–1450 (2006).
16. M. J. McGill, D. L. Hlavka, W. D. Hart, V. S. Scott, J. Spinhirne, and B. Schmid, "Cloud physics lidar: instrument description and initial measurement results," Appl. Opt. **41**(18), 3725–3734 (2002).
17. S. Ismail, E. V. Browell, R. A. Ferrare, S. A. Kooi, M. B. Clayton, V. G. Brackett, and P. B. Russell, "LASE measurements of aerosol and water vapor profiles during TARFOX," J. Geophys. Res. **105**(D8), 9903–9916 (2000).
18. C. J. Grund, R. M. Banta, J. L. George, J. N. Howell, M. J. Post, R. A. Richter, and A. M. Weickmann, "High-Resolution Doppler Lidar for Boundary Layer and Cloud Research," J. Atmos. Ocean. Technol. **18**(3), 376–393 (2001).
19. S. Y. Matrosov, B. W. Orr, R. A. Kropfli, and J. B. Snider, "Retrieval of vertical profiles of cirrus cloud microphysical parameters from Doppler radar and infrared radiometer measurements," J. Appl. Meteorol. **33**(5), 617–626 (1994).
20. G. G. Mace, T. A. Ackerman, P. Minnis, and D. F. Young, "Cirrus layer microphysical properties derived from surface-based millimeter radar and infrared interferometer data," J. Geophys. Res. **103**(D18), 23207–23216 (1998).
21. Z. Wang, and K. Sassen, "Cirrus cloud microphysical property retrieval using lidar and radar measurements: I algorithm description and comparison with in situ data," J. Appl. Meteorol. **41**(3), 218–229 (2002).
22. Z. Wang, K. Sassen, D. Whiteman, and B. Demoz, "Studying altocumulus plus virga with ground-based active and passive remote sensors," J. Appl. Meteorol. **43**(3), 449–460 (2004).
23. D. P. Donovan, and A. Van Lammeren, "Cloud effective particle size and water content profile retrievals using combined lidar and radar observations, 1. Theory and examples," J. Geophys. Res. **106**(D21), 27425–27448 (2001).
24. H. Okamoto, S. Iwasaki, M. Yasui, H. Horie, H. Kuroiwa, and H. Kumagai, "An algorithm for retrieval of cloud microphysics using 95-GHz cloud radar and lidar," J. Geophys. Res. **108**(D7), 4226 (2003).
25. J. Delanoë, and R. J. Hogan, "A variatioanl scheme for retrieving ice cloud properties from combined radar, lidar, and infrared radiometer," J. Geophys. Res. **113**(D7), 7204 (2008), doi:10.1029/2007JD009000.
26. K. Sassen, "The polarization lidar technique for cloud research: a review and current assessment," Bull. Am. Meteorol. Soc. **72**(12), 1848–1866 (1991).
27. Z. Wang, and K. Sassen, "Cloud type and macrophysical property retrieval using multiple remote sensors," J. Appl. Meteorol. **40**(10), 1665–1683 (2001).
28. J. Klett, "Stable analytical inversion solution for processing lidar returns," Appl. Opt. **20**(2), 211 (1981).
29. J. D. Lindberg, W. J. Lentz, E. M. Measure, and R. Rubio, "Lidar determinations of extinction in stratus clouds," Appl. Opt. **23**(13), 2172–2177 (1984).
30. E. W. Eloranta, "Practical model for the calculation of multiply scattered lidar returns," Appl. Opt. **37**(12), 2464–2472 (1998).
31. J. D. Spinhirne, R. Boers, and W. D. Hart, "Cloud Top Liquid Water from Lidar Observations of Marine Stratocumulus," J. Appl. Meteorol. **28**(2), 81–90 (1989).
32. Y. Hu, M. Vaughan, Z. Liu, B. Lin, P. Yang, D. Flittner, B. Hunt, R. Kuehn, J. Huang, D. Wu, S. Rodier, K. Powell, C. Trepte, and D. Winker, "The depolarization - attenuated backscatter relation: CALIPSO lidar measurements vs. theory," Opt. Express **15**(9), 5327–5332 (2007).
33. S. A. Young, "Analysis of lidar backscatter profiles in optically thin clouds," Appl. Opt. **34**(30), 7019–7031 (1995).
34. J. D. Locatelli, and P. V. Hobbs, "Fall speeds and masses of solid precipitation particles," J. Geophys. Res. **79**(15), 2185–2197 (1974).

1. Introduction

Clouds couple the Earth's water and energy cycles and are an important component of our climate system [1]. Estimates of global warming due to doubled CO_2 range from 1.3 K to 5.4

#110893 - $15.00 USD Received 4 May 2009; revised 19 Jun 2009; accepted 19 Jun 2009; published 23 Jul 2009

K across General Circulation Models (GCMs) [2]. This large range can be attributed to differences in cloud parameterizations from different GCMs due in part to our limited understanding of clouds [3,4]. Improving our understanding of cloud microphysical processes and dynamics is regarded as a high priority in current weather and climate research [5–8].

Airborne cloud observations have always played an important role in advancing our understanding of cloud microphysics and dynamics and will continue to do so in the future. Compared with ground- and space-based remote sensing, current in situ sampling can provide a variety of direct measurements including traditional meteorological parameters, comprehensive cloud properties, aerosol physical and chemical properties, and atmospheric trace gases. However, these detailed measurements are only available along the flight path of the aircraft, typically at a single altitude. For many physical process studies, vertical profiles are needed. To study the development of drizzle in marine stratocumulus clouds it is ideal to have the vertical profiles of liquid water content, effective radius of water droplets, drizzle size, and their horizontal variability. Airborne in situ sampling is also severely limited by small sample volumes. For example, in situ cloud probes only have sampling volumes ranging from ~40 to ~10^4 cm^3 s^{-1} for large to small hydrometeors, respectively. These small sample volumes make it difficult to study atmospheric properties with strong spatial inhomogeneities or to detect early onset of precipitation particles in clouds.

Although not as detailed (such as cloud droplet size distribution) as in situ sampling, airborne remote sensing provides a set of measurements that can be obtained neither through in situ techniques nor through ground-based remote sensors. Airborne vertical profiling capabilities are mainly provided by active sensors, such as lidar and radar. Airborne radars provide measurements of cloud, precipitation, and cloud scale dynamics [9–11], and have proved invaluable for gaining insights of mechanisms within convective cloud systems and hurricanes [12], marine Sc clouds [13,14], and cumulus clouds [15]. Lidars operate at a much shorter wavelength than radars and have capabilities to measure clouds [16], aerosol, trace gases [17], and wind [18]. Airborne passive sensors are also widely used in field campaigns, and although they can be used to retrieve temperature and water vapor profiles, these profiles are limited to coarse vertical resolutions. Due to the motion of the aircraft, airborne remote sensors are capable of providing 2-D and 3-D measurements.

The integration of airborne in situ sampling and remote sensing provides new observational capabilities to study atmospheric processes. For example, 2-D cross-sections of cloud microphysical properties retrieved from active remote sensor measurements provide a context to understand detailed in situ cloud measurements. The integration of in situ and remote sensing can be achieved with one or more aircraft in a field campaign. The NASA Cirrus Regional Study of Tropical Anvils and Cirrus Layers-Florida Area Cirrus Experiment (CRYSTAL-FACE, http://www.espo.nasa.gov/crystalface/) in 2002 is a great example of multiple-aircraft synergy. With two dedicated remote sensing aircraft, two additional aircraft focused on in situ measurements, and carefully coordinated flights, CRYSTAL-FACE provided a comprehensive data set to study convectively generated anvil clouds. However, such multiple-aircraft field campaigns are very expensive and require a high degree of coordination. Additionally, it is extremely difficult to collocate measurements from multiple aircraft in both space and time. Thus, integration of in situ sampling and remote sensors on a single aircraft provides an avenue that is important both from an economic and logistical point of view.

The University Wyoming King Air (UWKA) has been used to obtain in situ measurements in clouds for over 30 years. Beginning in 1992 and continuing throughout the 1990's, the group at the University of Wyoming worked to develop an integrated in situ/remote sensing platform for use in cloud studies [13]. The Wyoming Cloud Radar (WCR), an airborne 94 GHz cloud radar, continues to be a key instrument for cloud studies on both the UWKA and NSF/NCAR C130. Over the last 17 years the WCR evolved from an initial single beam sensor to simultaneously selectable multiple beam configurations to provide measurements of cloud

#110893 - $15.00 USD Received 4 May 2009; revised 19 Jun 2009; accepted 19 Jun 2009; published 23 Jul 2009

structure and dynamics [15]. For example, the WCR can provide a profile both above and below the aircraft in a two-dimensional "curtain" that provides a context to analyze in situ detail microphysical measurements. However, WCR measurements only provide limited information on cloud microphysical properties, especially, for mixed-phase clouds or water clouds with drizzle.

Experiments utilizing ground-based observations [19–24] have demonstrated the effectiveness of integrating lidar, radar and radiometer observations to better determine cloud microphysical properties. Wang and Sassen [21] showed that reliable ice water content (IWC) and general effective radius (D_{ge}) profiles can be retrieved from lidar and cloud radar measurements. Similar integrated observations are now available from airborne platforms, such as the high-altitude NASA ER-2 aircraft. The NASA A-train satellites combine active and passive sensor measurements to provide more reliable cloud properties globally [6,25]. A multi-sensor cloud remote sensing capability from the UWKA will allow investigators to effectively combine vertical profiles of cloud properties together with detailed in situ data to better study cloud microphysical properties and processes. The Wyoming Cloud Lidar (WCL) is designed to achieve such a goal by providing high spatial resolution cloud base measurements from the UWKA, as well as cloud and aerosol extinction coefficient and depolarization profiles. Together with the existing cloud-scale dynamics observation capabilities of the WCR, combining WCR, WCL and in situ sampling from the UWKA will provide improved measurements for cloud microphysics and dynamics studies.

The WCL has been successfully deployed (zenith pointing) on the UWKA during the Wyoming Airborne Integrated Cloud Observations Experiment (WAICO) in 2008 and 2009, the Cloud GPS experiment in 2008 and on the NSF/NCAR C-130 during the Ice Clouds Experiment-Layer Clouds (ICE-L) in 2007 and the VAMOS Ocean-Cloud-Atmosphere-Land Study (VOCALS) in 2008. These experiments demonstrated the value of the WCL for airborne cloud and aerosol measurements. This paper provides an overview of the WCL system and its capabilities. The WCL system description is given in Section 2. The WCL measurements capabilities and applications are illustrated with measurement examples in Section 3. And in Section 4 we provide a brief conclusion.

2. The WCL system specification

The WCL, a compact elastic lidar with depolarization measurements, is designed to work together with the WCR to provide more comprehensive cloud macrophysical and microphysical measurements from the UWKA and NSF/NCAR C-130 aircraft. Because of limitations on both space and power available on the UWKA the WCL cannot use a large telescope or high power laser typically used by lidars on larger aircraft. In order to use one of the existing upward fuselage ports for the WCL, a small telescope combined with a relatively high pulse-energy laser is used. This combination provides the needed sensitivity for cloud and aerosol measurements. System specifications are summarized in Table 1.

#110893 - $15.00 USD Received 4 May 2009; revised 19 Jun 2009; accepted 19 Jun 2009; published 23 Jul 2009

Table 1. WCL System Parameters

Transmitter	
Laser Wavelength	355 nm Nd:YAG
Pulse Repetition Frequency	20 Hz
Pulse width	~8 ns
Pulse Energy	16 mJ
Receiver	
Diameter	~75 mm
Field of view	300 to 2000 μrad
Data System	
Number of Channels	Two
Detector	PMT
Range Resolution	3.75m, 7.5m, 15m, 30m (programmable)
Maximum Range	30 km
Data acquisition system	Combined analog and photon counting system from LICEL, GmbH

With the size, pulse energy and eye safety of the laser in mind, an Ultra Pulsed Nd:YAG Laser from the Big Sky Laser Technologies, Inc, providing a 20 Hz 16 mJ output at 355 nm, is used for the WCL. Operating at 355 nm not only makes it easy to achieve eye safe operation, it also provides a stronger molecular backscattering signal than a lidar operating at 532 or 1064 nm with the same laser energy. This is important for calibrating backscattering coefficients. The schematic diagram of the system is given in Fig. 1. The laser beam is expanded 5 times to a diameter of 15 mm before emittance into atmosphere, making the system eye safe beyond a distance ~65 m. To improve lidar linear depolarization measurements, a 1/2 λ wave plate is placed after the beam expander and this is coupled with a cubic polarization beam splitter in the receiver path.

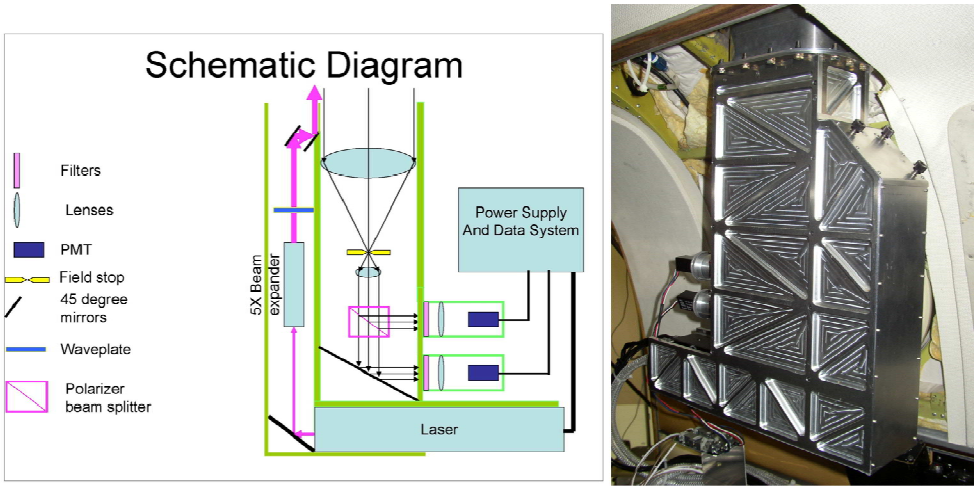

Fig. 1. WCL system diagram and its zenith pointing installation photo on the UWKA

The receiver is based on 75mm refractive lens with 12.5mm collimated beam that enters into the cubic polarization beam splitter. The field of view is controlled by a pin hole located at the focal plane of the receiving lens. The PMT packages include narrow band filters (0.3

#110893 - $15.00 USD Received 4 May 2009; revised 19 Jun 2009; accepted 19 Jun 2009; published 23 Jul 2009

nm), a focus lens, and a compact PMT. To provide needed ruggedness and stability for WCL to operate in a vibration environment, the receiver is designed to share the same optical bench with the transmitter. The gain of the PMT can be easily adjusted with bias control voltage. Signals from the PMTs are sent to the LICEL data acquisition system. The data system has a combined A/D and photon counting capability. To provide high spatial measurements, only strong signals digitized by A/D at 40 MHz are saved at single shot or averaging of number of shots. Thus, the WCL can provide measurements at ~4.5 m horizontal and 3.75 m vertical resolutions from the UWKA (average cruise speed of ~90 m/s).

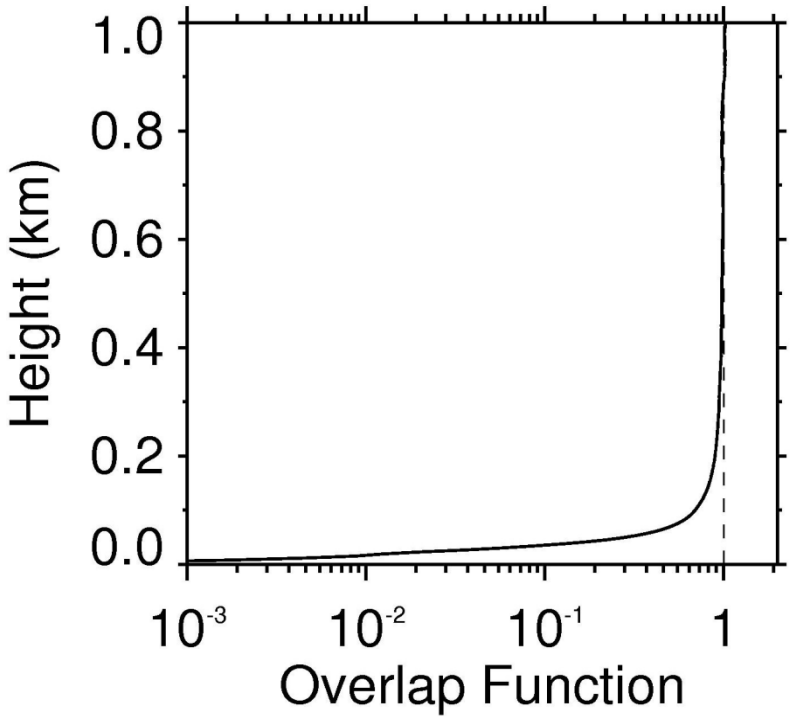

Fig. 2. The overlap function of the WCL during the ICE-L experiment.

To effectively combine WCR and WCL measurements with in situ sampling, an important design goal of the WCL is to provide measurements as close to the aircraft as possible. However, near end strong lidar signals, especially in clouds, have potential to saturate the detectors. The WCL was designed with this tradeoff in mind. The resulting WCL overlap function, which was determined based on molecular signals collected above the boundary layer, during the ICE-L experiment is shown in Fig. 2. The WCL has a full overlap at ~600m but still can provide measurements as close as 20 m from aircraft. Although the overlap function can be optimized to effectively minimize near end signals, near end signals can still saturate when the aircraft is flying through dense clouds. As examples presented in the following Section, the WCL can provide high signal-to-noise-ratio measurements of cloud and aerosol within 1-2 km of the aircraft. Averaging vertically and horizontally can improve the signal-to-noise-ratio when needed.

#110893 - $15.00 USD Received 4 May 2009; revised 19 Jun 2009; accepted 19 Jun 2009; published 23 Jul 2009

3. Applications

3.1 Cloud phase discrimination

Cloud water phase, liquid, ice or mixed-phase, is an important cloud property affecting cloud radiative forcing, and controlling cloud microphysical evolution. Multiple remote sensor cloud retrievals often require a priori knowledge of cloud phase to apply proper microphysical assumptions. In order to interpret in situ measurements of cloud properties at flight altitude it is critical to know the vertical cloud phase structure. For example, ice crystals grow much fast in mixed-phase clouds than in ice clouds. Lidar linear depolarization ratio (LDR) can be used effectively for cloud phase identification [26,27]. An example of WCL measurements for cloud phase discrimination is given in Fig. 3. Liquid or liquid-dominated mixed-phase regions are indicated by strong backscattering powers and small LDR. The ice phase cloud beneath the liquid dominated mixed-phase layer is indicated by weak power and large LDR. For this wave cloud, ice crystals are generated in the mixed-phase layer (lidar signals are dominated by supercooled water), then fall out of the layer as they grow big quickly under mixed-phase conditions. With this phase discrimination capability, we can see the ice evolution in this wave cloud.

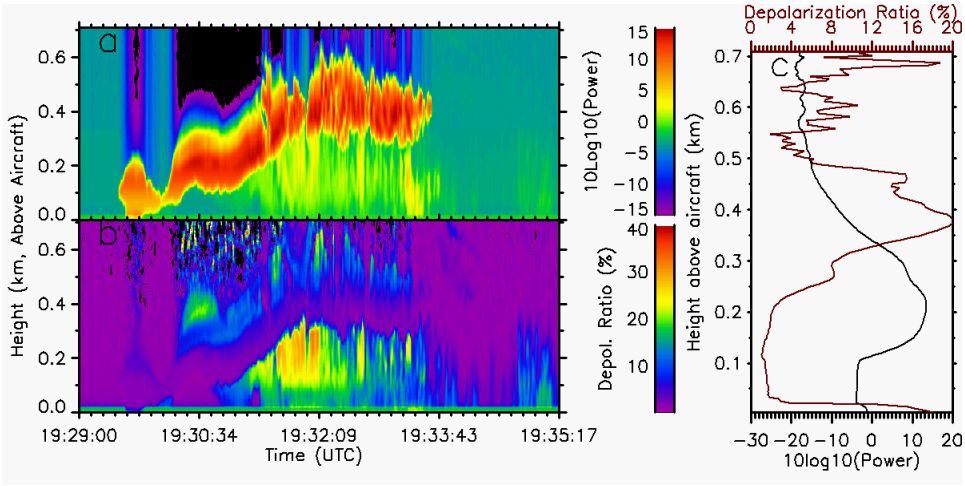

Fig. 3. WCL measurements of a wave cloud: range corrected attenuated backscattering power (a), lidar linear depolarization ratio (b), and profiles of both at time 19:30:34 UTC (c). The horizontal wind direction is from left to right.

Phase discrimination relies on the facts that ice crystals return a high LDR and water droplets return low LDR. Two situations limit the effectiveness of using LDR to provide cloud phase profiles. The first is caused by strong multiple scattering in water clouds. Although liquid water clouds normally have very small LDR near cloud base, LDR linearly increases with height due to multiple scattering as shown in Fig. 3(c). Under this situation, water phase can best be identified by combining the LDR profile, which is small near cloud base and increase with height from the base, with strong signal intensity. The second situation is caused by ice crystal orientation. Ice crystals normally produce high LDR, but horizontally orientated plates can produce very low LDR and strong backscattering. Therefore, to better identify cloud phase, LDR measurements need to be combined with lidar signal intensity as well as attenuation.

Most water clouds cannot be fully penetrated by the lidar, thus cloud top height is uncertain in this situation, such as during the period around 19:30:34 UTC. Figure 3(c) presents an example (4-shot average) to show WCL noise level, which is around −18 dB during the ICE-L experiment. Considering molecular signal (as seen below 100 m) of −4 dB

#110893 - $15.00 USD Received 4 May 2009; revised 19 Jun 2009; accepted 19 Jun 2009; published 23 Jul 2009

and cloud peak signal of 12 dB, signal-to-noise ratios of WCL signals for short-range cloud targets are good to provide cloud retrievals at high spatial resolutions.

3.2 Boundary layer aerosol measurements

Although the WCL is mainly designed for cloud measurements, it is sensitive enough for boundary layer aerosol measurements as well. Atmospheric aerosols are mainly concentrated in the atmospheric boundary layer and can strongly affect the atmospheric energy budget through both direct and indirect effects. Uncertainties due to aerosol forcing represent the single largest uncertainty in the forecast of climate change. Key to unraveling the mystery of aerosol direct effect is to better understand large spatial and temporal variations in both concentration and composition of aerosol. Airborne in situ and remotely sensed aerosol measurements provide data to understand these variations. Figure 4 presents an aerosol structure observed by the WCL within a strong inversion-topped marine boundary layer over the eastern edge of the South Pacific during the VOCALS campaign. The boundary layer aerosol is well mixed up to 300 m as indicated by attenuated backscattering coefficient. Sea salt aerosols under high relative humidity conditions exist as liquid particles and produce low depolarization. Figure 4 shows that aerosol backscattering decreases significantly within the top 100 m of the boundary layer due to entrainment mixing of dry and warm free tropospheric air with moister boundary layer air. With the decrease of relative humidity near the top of the boundary layer, the size of sea salt aerosol decreases. The narrow band of high depolarization aerosols around 400 m indicates the sea salt crystals have formed in a region where relative humidity drops below the recrystallization point. The thickening of the layer around 17:05:30 UTC indicates stronger entrainment processes in the region compared with nearby regions. These aerosol features suggest that high spatial resolution aerosol measurements from airborne active remote sensing can provide a new way to study mixing processes in inversion topped boundary layers. Although, the shallow marine boundary layer is well mixed, the backscattering signal indicates noticeable horizontal inhomogeneity.

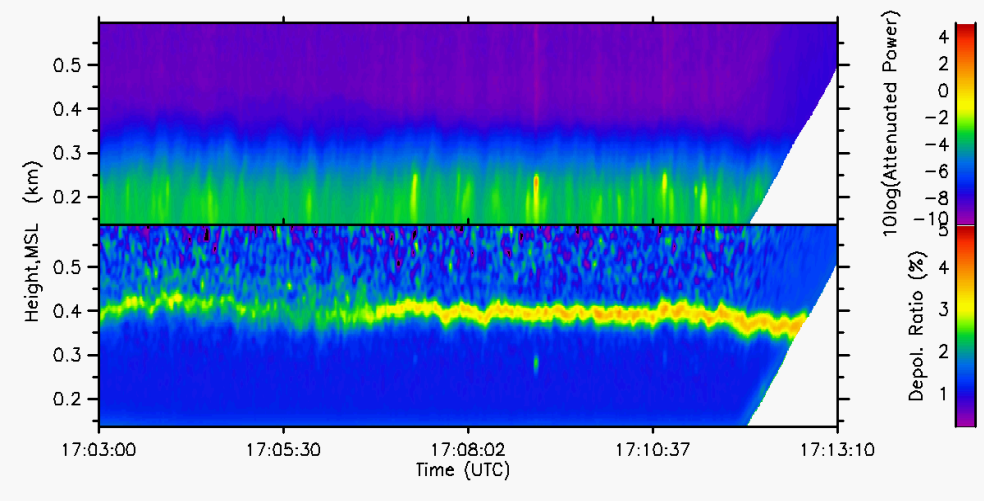

Fig. 4. WCL measurements of a marine boundary layer aerosol structure: attenuated backscattering power (top) and lidar linear depolarization ratio (bottom).

Aerosol activation as cloud condensation nuclei or ice nuclei is a necessary step for cloud formation. Figure 5 shows a WCL measurement example of both aerosol and cloud in a convective marine boundary layer. Clouds in Fig. 5 are shown in white and beneath the clouds aerosol “plumes” rising from lower levels are evident. Cloud base heights generally indicate local lifting condensation levels. The cloud base height variation given in Fig. 5 is suggestive

#110893 - $15.00 USD Received 4 May 2009; revised 19 Jun 2009; accepted 19 Jun 2009; published 23 Jul 2009

of significant near surface water vapor inhomogeneity. The increase of aerosol backscattering intensity near cloud base is due to the hydroscopic growth of aerosols. The vertical profiles of aerosol and clouds together with aircraft in situ data provide a more powerful way to study the linkages of aerosol, water vapor, clouds, and dynamics to advance our understanding of cloud microphysical physics.

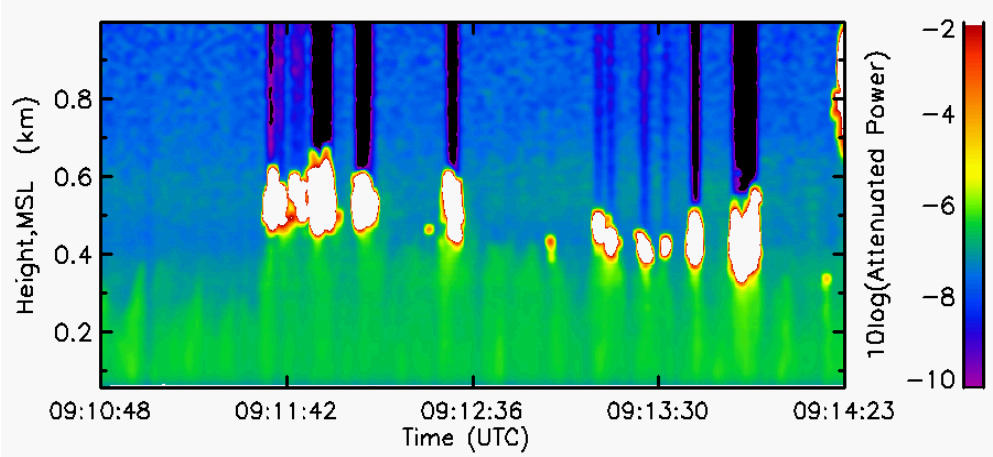

Fig. 5. WCL measurements of boundary layer aerosol and clouds during the VOCALS campaign.

3.3 Cloud optical and microphysical properties measurements

Cloud extinction coefficient can be retrieved from WCL measurements based on the backward solution of the lidar equation [28,29]. The greatest challenge for cloud extinction retrieval is accounting for multiple scattering. The impact of multiple scattering on the lidar return signal mainly depends on the cloud extinction, droplet size, and receiver field-of-view [30]. Water clouds are typically optically thick with strong multiple scattering that effects the lidar signals as indicated in Fig. 3. Due to the regular shape of water droplets, lidar multiple scattering in water clouds can be modeled relatively easily compared to ice clouds and thus can be corrected in several different ways. Based on airborne lidar measurements, Spinhirne et al. [31] demonstrated an approach to retrieve cloud extinction coefficient of stratus and Sc clouds in the presence of multiple scattering using an effective backscatter to extinction ratio. A recent study by Hu et al. [32] shows a robust relationship between LDR and multiple scattering contribution in water clouds, that can be used to correct multiple scattering effects for extinction retrievals. Compared to water clouds, ice clouds are optically thin reducing problems associated with multiple scattering, especially for short range measurements and small fields of view. For many ice clouds, the use of the total optical depth derived from the molecular signal above the cloud layer provides a constraint [33] to improve the retrievals. An example of retrieved ice cloud extinction profiles (based on 4-shot averaged measurements) for a cirrus generation cell is presented in Fig. 6(c).

To fully characterize cloud radiative impact and to study cloud microphysical processes, it is important to determine profiles of cloud microphysical properties such as water content and hydrometeor size. Although cloud microphysical properties can be estimated from single instrument measurements, they can be retrieved with improved accuracy by combining multiple sensor measurements [20–25]. Because the WCR (λ~3160 μm) and WCL (λ~0.355 μm) make measurements at such different wavelengths, their response to these microphysical cloud properties differs significantly. Combined WCL and WCR measurements can provide information about cloud particle size, beyond the sum of what each individual instrument provides. WCR radar reflective factor (Z_e) is proportional to the sixth power of particle

#110893 - $15.00 USD Received 4 May 2009; revised 19 Jun 2009; accepted 19 Jun 2009; published 23 Jul 2009

diameter when the scattering is within the Rayleigh scattering regime. Thus, Z_e and the WCR measurements are more sensitive to larger particles. On the other hand the WCL backscattering intensity is only proportional to the second power of particle diameter, thus it is more sensitive to smaller particles. For ice clouds, ice water content (IWC) and general effective radius (D_{ge}) can be reliably estimated from WCL and WCR measurements [21].

#110893 - $15.00 USD Received 4 May 2009; revised 19 Jun 2009; accepted 19 Jun 2009; published 23 Jul 2009

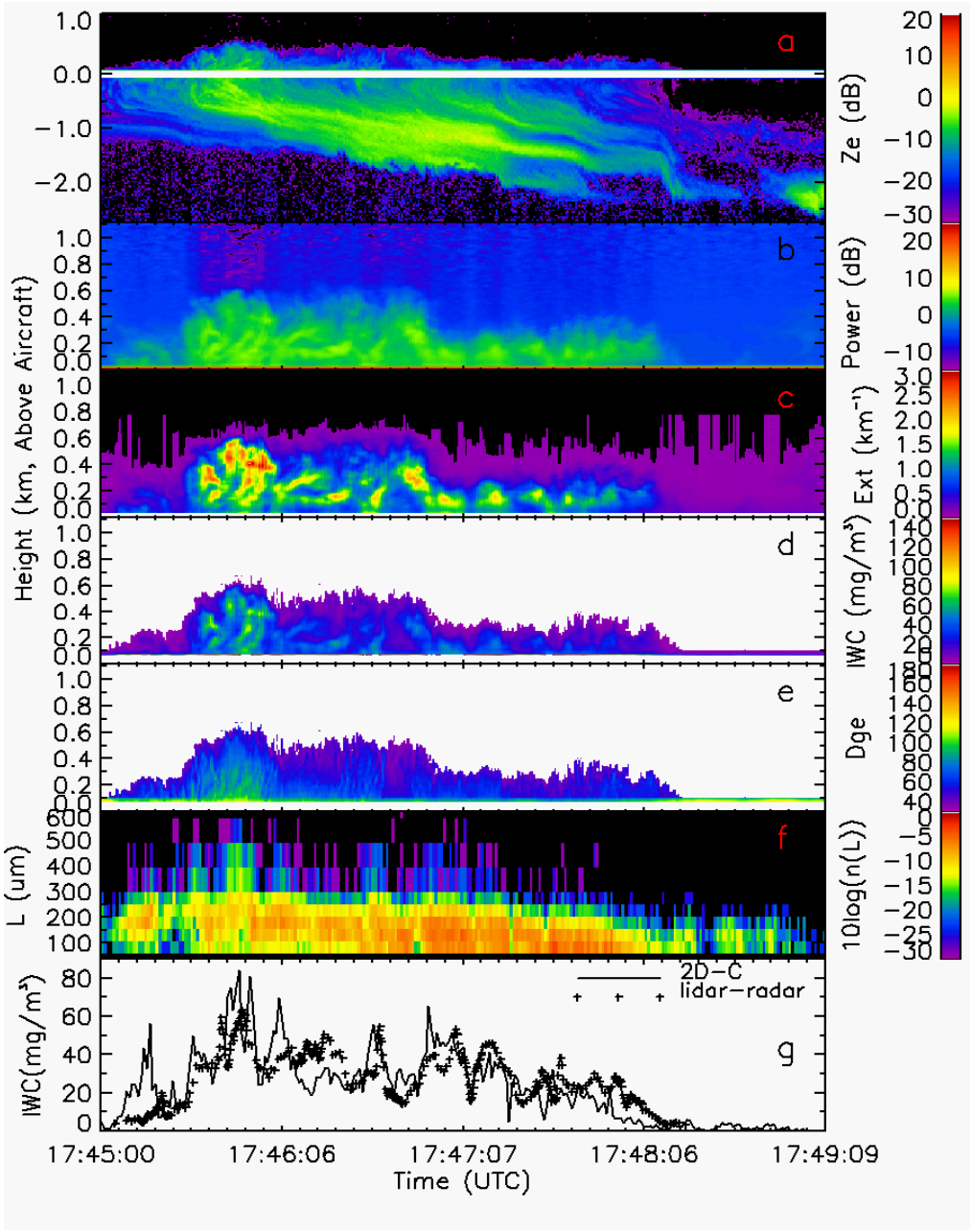

Fig. 6. Combined WCR and WCL measurements of ice clouds and microphysical properties retrievals: a) up and down WCR reflectivity factor, b) upward WCL attenuated backscattering power, c) WCL retrieved cloud extinction coefficient, d) retrieved IWC profile, f) retrieved D_{ge} profile, f) 2D-C measure ice crystal size distribution in terms of maximum length (number/L/um), and g) comparison of 2D-C estimated IWC with retrieved IWC at ~100m above the King Air.

An example of retrieved IWC and D_{ge} profiles based on combined WCR and WCL measurements is given in Figs. 6(d) and 6(f). IWC profiles reveal fine structure of ice generation within the generation cell (~17:45:55) while D_{ge} profiles show a general vertical

#110893 - $15.00 USD Received 4 May 2009; revised 19 Jun 2009; accepted 19 Jun 2009; published 23 Jul 2009

pattern of ice particle size: increasing size with decreasing altitude. However, there are large variations in D_{ge} values horizontally. These remote sensing cloud microphysical properties can be compared with in situ data. Figure 6(f) shows ice crystal number concentration as a function of ice crystal maximum length L from the 2D-C probe. A large horizontal variation of ice crystal size distribution at the flight altitude is clear from 2D-C measurements and is consistent with WCR and WCL retrievals. Although the 2D-C cannot provide IWC directly, IWC can be estimated from measured size distributions based on mass-length relationships and ice crystal shapes. Estimated IWC assuming mixtures of unrimed aggregate plates, bullets and columns [34] is presented in Fig. 6(g). For comparison, WCR and WCL retrievals at ~100m above the flight altitude are also shown in Fig. 6(g). Apparently, the two IWCs agree well, but there are periods with large differences. This can likely be attributed to the vertical spatial inhomogeneity of IWC as shown in Fig. 6(d).

4. Conclusion

The WCL, a compact two-channel elastic lidar, has been successfully built to work together with the WCR on UWKA and NSF/NCAR C-130 aircraft. By using a compact laser operating at 355 nm and 16 mJ, the WCL can provide eye safe operation as well as needed sensitivities for cloud and aerosol measurements. The WCL has been deployed in four field projects under a variety of atmospheric and cloud conditions during the past two years. Throughout these campaigns, it has exhibited the needed reliability for turn-key operation from aircraft. Although, the WCL has no automatic bore sight mechanism, the WCL is stable enough to hold its alignment for an entire campaign due to the unique design in which the same optical bench is shared by the receiver and the transmitter. To provide effective synergy with in situ measurements, the WCL can provide near range measurements as close as 20 m.

WCL measurement examples are provided to illustrate the measurements capability of the instrument. WCL linear depolarization ratio measurements provide important information for cloud phase discrimination, especially when combined with backscattering intensity. Cloud extinction coefficient can also be retrieved from WCL measurements although one needs to properly account for multiple scattering effects in water clouds by using an effective backscatter to extinction ratio or LDR measurements. The WCL is sensitive enough to provide high spatial resolution measurements of boundary layer aerosols which in turn provides new opportunities for boundary layer process and cloud and aerosol studies.

New cloud observation capabilities can be achieved by combining WCR and WCL measurements. Due to their different sensitivities over the range of hydrometeors in clouds, combined WCR and WCL measurements can provide improved estimates of cloud microphysical properties. An example of a microphysical retrieval from an ice cloud is presented. For mixed-phase clouds and drizzling liquid water clouds, the WCR can provide ice particle or drizzle drop information while WCL measurements will be dominated by cloud water droplets. Combined, this allows a better characterization of these clouds. Furthermore, combined WCR and WCL measurements also can provide improved measurements of cloud boundaries. The synergy of WCL and WCR measurements with in situ sampling from an aircraft provide a unique set of measurements for compiling better statistics for comparisons between in situ and retrieved microphysical properties and an effective way to observe and understand the evolution of cloud microphysical properties.

Acknowledgments

This research is supported by NSF under award of ATM 0645644 and ATM 0745986 and University of Wyoming. The UWKA is supported by NSF award ATM 0334908. The authors would like to thank the UWKA and NCAR C-130 team for their efforts in collecting WCL data.

#110893 - $15.00 USD Received 4 May 2009; revised 19 Jun 2009; accepted 19 Jun 2009; published 23 Jul 2009